

RESEARCH ARTICLE

10.1002/2016WR020014

Key Points:

- Crustal fluxes are often invoked to explain groundwater helium in excess of steady state local production
- The relationship between $^{234}\text{U}/^{238}\text{U}$ activity ratios and ^4He contents suggests a common process releasing ^{234}U and ^4He into groundwater locally
- Modeling ^4He release from comminuted grains after glaciation-induced fracturing could explain local ^4He excesses in groundwater

Correspondence to:

P. Méjean,
mejeanpauline@gmail.com

Citation:

Méjean, P., D. L. Pinti, B. Ghaleb, and M. Larocque (2017), Fracturing-induced release of radiogenic ^4He and ^{234}U into groundwater during the last deglaciation: An alternative source to crustal helium fluxes in periglacial aquifers, *Water Resour. Res.*, 53, 5677–5689, doi:10.1002/2016WR020014.

Received 26 OCT 2016

Accepted 16 JUN 2017

Accepted article online 19 JUN 2017

Published online 13 JUL 2017

Fracturing-induced release of radiogenic ^4He and ^{234}U into groundwater during the last deglaciation: An alternative source to crustal helium fluxes in periglacial aquifers

Pauline Méjean^{1,2} , Daniele L. Pinti¹ , Bassam Ghaleb¹, and Marie Larocque¹ 

¹GEOTOP and Département des sciences de la Terre et de l'atmosphère, Université du Québec à Montréal, Montréal, Quebec, Canada, ²Now at Laboratoire de développement Analytique Nucléaire Isotopique et Élémentaire, CEA, Saclay, France

Abstract External ^4He sources have been invoked to explain ^4He concentrations in groundwater greater than those expected from in situ U and Th production. In a fractured aquifer of Ordovician age located in the St. Lawrence Lowlands (Quebec, Canada), ^4He concentrations of up to $4.48 \times 10^{-5} \text{ cm}^3 \text{ STP g}_{\text{H}_2\text{O}}^{-1}$ were measured. Such concentrations are ~ 1000 times higher than would be expected from in situ production. A concomitant increase in ^4He concentration and $^{234}\text{U}/^{238}\text{U}$ activity ratio is shown, suggesting a common release process in groundwater for ^{234}U and ^4He . This process has tentatively been identified as glaciation-induced rock fracturing following the Laurentide Ice Sheet retreat. The resulting increase in exposed grain surface facilitates ^{234}U release by α -recoil and that of radiogenic ^4He by diffusion. Using a model of helium diffusion from a spherical grain, it is shown that rock fracturing facilitated the release of accumulated ^4He at rates ranging from 4.2×10^{-10} to $1.06 \times 10^{-8} \text{ cm}^3 \text{ STP g}_{\text{H}_2\text{O}}^{-1} \text{ yr}^{-1}$. These release rates are between 1000 and 30,000 times higher than the local U and Th steady state production rate, of $3.5 \pm 1.4 \times 10^{-13} \text{ cm}^3 \text{ STP g}_{\text{rock}}^{-1} \text{ yr}^{-1}$. Integration of ^4He release rates over time yields a radiogenic ^4He concentration of between 3.85×10^{-6} and $7.12 \times 10^{-5} \text{ cm}^3 \text{ STP g}_{\text{H}_2\text{O}}^{-1}$, in the range of concentrations measured in the St. Lawrence Lowlands fractured aquifers. Results support the occurrence of a local radiogenic helium source to explain the excesses measured in groundwater without requiring a significant external He crustal flux.

1. Introduction

Groundwater is the largest reservoir of freshwater available for human use. Of the 22.6 Mkm³ of groundwater contained within the first 2 km of the upper crust, less than 6% is modern groundwater (i.e., is less than 50 years in age) [Gleeson *et al.*, 2016]. The rest ranges from a few thousand [Aggarwal *et al.*, 2015] to potentially hundreds of millions of years in age [Bottomley *et al.*, 1984; Lippmann-Pipke *et al.*, 2011; Pinti *et al.*, 2011; Holland *et al.*, 2013]. Precisely constraining the age of the remaining volume of old groundwater is essential to evaluate these groundwater reservoirs, which will be increasingly solicited by the growing world population as modern groundwater becomes increasingly endangered by global change stresses.

Younger groundwater (less than 50 years old) can be precisely dated using $^3\text{H}/^3\text{He}$ [e.g., Tolstikhin and Kamenskiy, 1969]. Dating older groundwater is a challenge, because water-rock interaction alters the initial concentration of radionuclides [e.g., Phillips and Castro, 2003]. An example is ^{14}C (half-life = 5730 years), which is primarily introduced into groundwater in the soil zone through biological processes. Along the flow path, ^{14}C activity decreases according to radioactive decay [Plummer and Glynn, 2013]. However, exchange with carbonates [Fontes, 1992] and the addition of ^{14}C from old organic matter or CH₄ [Aravena *et al.*, 1995] can significantly alter the original ^{14}C activity, resulting in older apparent ages.

Radiogenic ^4He is the decay product of ^{238}U , ^{235}U , and ^{232}Th contained in rocks. The produced ^4He is transferred from rocks into groundwater mainly by diffusion and α -recoil [e.g., Torgersen, 1980]. Because of the inert nature of helium as a noble gas, and the long half-lives of the parent nuclides, the U-Th/ ^4He dating method can potentially be used to estimate groundwater ages ranging from a few hundred years to hundreds of millions of years [Marine, 1979; Andrews and Kay, 1983; Torgersen, 1980; Solomon *et al.*, 1996; Pinti *et al.*, 2011]. However, numerous studies [see e.g., Pinti and Marty, 1998; Phillips and Castro, 2003; Kulongoski and Hilton, 2011 for a review] report U-Th/ ^4He ages consistently older than the hydrogeological ages. This

difference, the so-called ^4He excess [e.g., *Torgersen and Clarke*, 1985], is interpreted as resulting from an additional source of radiogenic helium, external to the aquifer.

Torgersen and Clarke [1985] found that the ^4He excess in groundwater of the Great Artesian Basin of Australia was equivalent to the total crustal production of radiogenic ^4He beneath the basin. A basal flux of radiogenic helium entering the aquifers was found to be able to balance the total helium budget in groundwater. *Mazor* [1995], *Tolstikhin et al.* [1996], and *Lehmann et al.* [2003] contested this model, suggesting instead that aquifers have heterogeneous hydraulic conductivities, and that connate (stagnant) water might exist [*Pinti et al.*, 1997], accumulating large amounts of radiogenic helium. Freshwater mixed with stagnant water [*Tolstikhin et al.*, 1996] or pore water from low-permeability shales [*Tolstikhin et al.*, 2005] might cause the ^4He excesses.

In numerous glaciated granular aquifers, it was observed that ^4He was released into water at high rates, on the order of 300–600 times greater than those expected from local U and Th production [*Solomon et al.*, 1996]. These authors developed a model to demonstrate that only a portion of the ^4He produced (i.e., the portion located close to the surface of the aquifer grains) can be released at steady state by diffusion and/or α -recoil. During rock fracturing, the increased surface area of the grain exposed to water induces the rapid release of ^4He produced and accumulated in the rock, creating helium excess in groundwater.

Vautour et al. [2015] measured ^4He excesses of up to $4.48 \times 10^{-5} \text{ cm}^3 \text{ STP g}_{\text{H}_2\text{O}}^{-1}$ in groundwater circulating in the Ordovician-age-fractured aquifer of the Becancour watershed in the St. Lawrence Lowlands of Quebec (Canada). Measured helium content is about 1000 times higher than that expected from local production in rocks. *Vautour et al.* [2015] interpreted the helium excesses in groundwater as deriving from a crustal flux entering the bottom of the aquifer. Helium flux was estimated to be $0.1\text{--}2 \times 10^{-7} \text{ cm}^3 \text{ STP cm}^{-2} \text{ yr}^{-1}$ (i.e., tens to hundreds of times lower than the average continental crust flux of $3.3 \times 10^{-6} \text{ cm}^3 \text{ STP cm}^{-2} \text{ yr}^{-1}$) [*O'Nions and Oxburgh*, 1983].

Méjean et al. [2016] measured the $^{234}\text{U}/^{238}\text{U}$ activity ratios ($(^{234}\text{U}/^{238}\text{U})_{\text{act}}$ hereafter) in the groundwater of the same aquifer as *Vautour et al.* [2015]. Observed relationships between the $(^{234}\text{U}/^{238}\text{U})_{\text{act}}$, the lithology of the aquifers, and the alkalinity and the chemistry of water clearly indicated that U was sourced from the aquifer and ^{234}U - ^{238}U fractionation (i.e., $(^{234}\text{U}/^{238}\text{U})_{\text{act}} \gg 1$) was controlled locally by the ejection of ^{234}U into the water by α -recoil, while its parent element, ^{238}U , was firmly trapped in the solid phase. *Méjean et al.* [2016] found an inverse relationship between the $(^{234}\text{U}/^{238}\text{U})_{\text{act}}$ and the $^3\text{He}/^4\text{He}$ ratios: freshwater, devoid of radiogenic helium, shows an $(^{234}\text{U}/^{238}\text{U})_{\text{act}}$ of close to unity (i.e., at secular equilibrium); older groundwater is progressively enriched in radiogenic helium (i.e., the $^3\text{He}/^4\text{He}$ ratio decreases) and the $(^{234}\text{U}/^{238}\text{U})_{\text{act}}$ increases to as much as 6. This relationship calls for a local enrichment mechanism for both ^{234}U and ^4He , within the aquifer rather than an external source of helium as suggested by *Vautour et al.* [2015]. *Méjean et al.* [2016] suggested that the opening of new fractures might provide additional surfaces from which ^{234}U migrates by α -recoil and ^4He migrates by diffusion into water at high rates but did not quantify these processes.

Here the potential of the U-He relationship to identify radiogenic ^4He sources within aquifers is shown. These sources can resolve the radiogenic ^4He excess found in groundwater without requiring significant crustal fluxes. It is shown that in periglacial aquifers, glaciation-induced fracturing results in high helium release rates, providing a dominant ^4He input in the aquifer. Helium and uranium data from *Méjean et al.* [2016] and *Vautour et al.* [2015] are revisited and integrated in a coupled model of ^{234}U - ^{238}U fractionation and radiogenic ^4He release into groundwater by glaciation-induced fracturing, using equations developed by *Andrews et al.* [1982] and *Solomon et al.* [1996].

2. Hydrogeology and Water Chemistry

The hydrogeological setting of the Becancour River watershed (2859 km²; Figure 1) in the St. Lawrence Lowlands is briefly described here to highlight the context of this work. Details can be found in *Larocque et al.* [2013], *Vautour et al.* [2015], and *Méjean et al.* [2016]. The regional aquifer of the Becancour River watershed is mainly composed of fractured Ordovician carbonate-shale deposits belonging to the St. Lawrence Platform [*Larocque et al.*, 2013]. Recharge to this aquifer occurs in the Appalachian Mountains, where Cambrian to Devonian siliclastic and metasedimentary rocks (shales and schists) outcrop [*Larocque et al.*, 2013]. Unconsolidated Quaternary fluvio-glacial, deltaic, and lacustrine sands (Lobtinière and Vieilles Forges sands) are found in the middle and downstream portions of the Becancour River watershed [*Godbout*, 2013]. These deposits create granular aquifers of limited extent and thickness, partially buried under deposits of marine

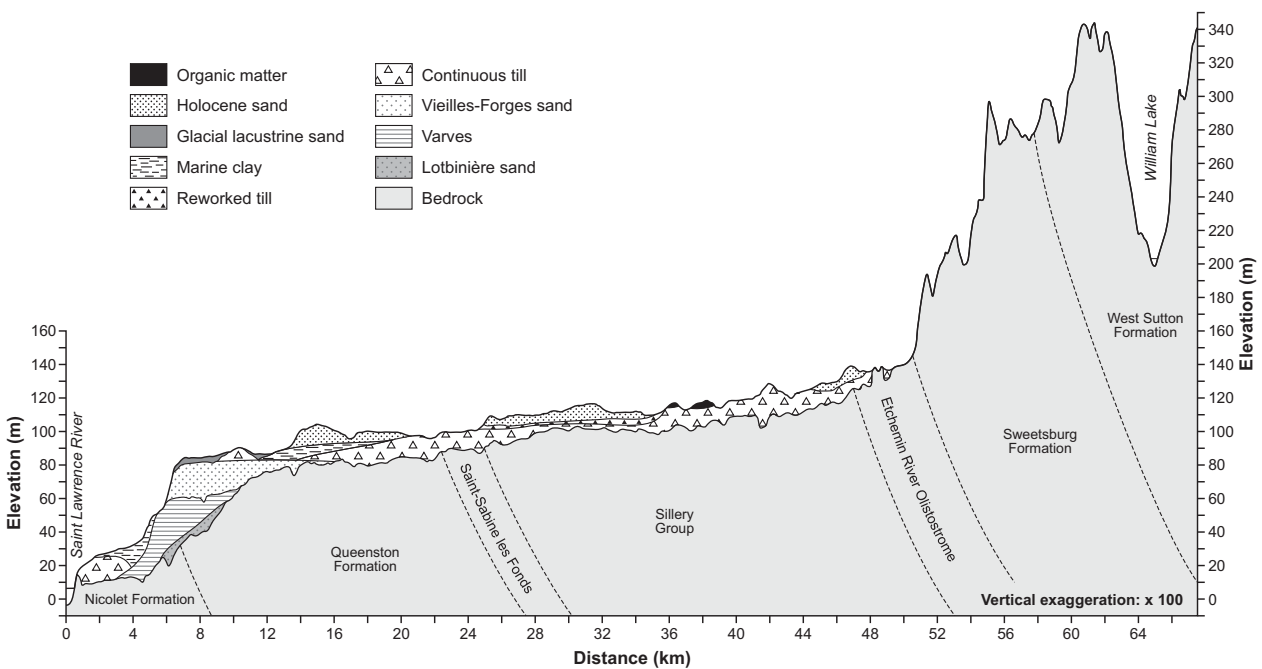
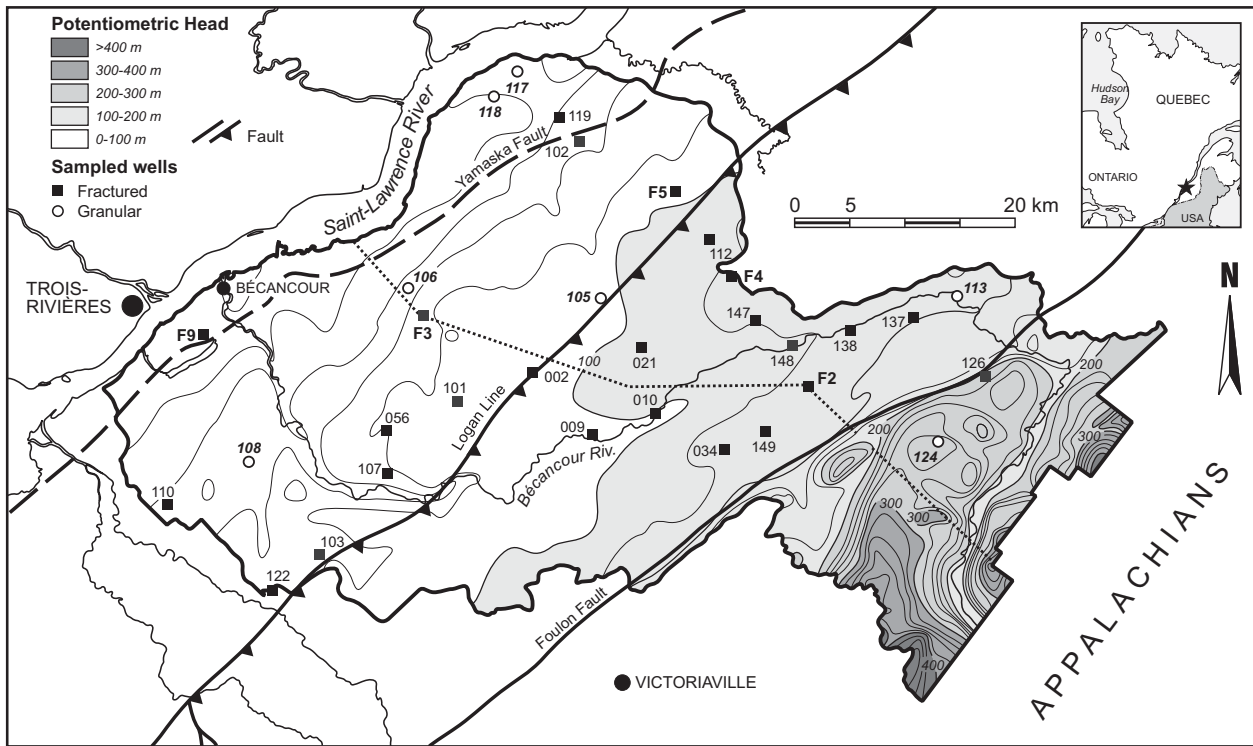


Figure 1. (a) Map of the Becancour watershed. Potentiometric head contour lines of the fractured bedrock aquifer, and locations of groundwater samples are indicated and (b) cross section of the Quaternary and Ordovician aquifers. Geological formations and groups of the St. Lawrence Platform and of the Appalachian Mountains are illustrated. Both figures are modified from Larocque et al. [2013].

clay. These clay deposits are the result of marine transgression-regression cycles caused by the marine Champlain Sea invasion, dated at 9750 B.P. [Occhietti et al., 2001].

Groundwater flows regionally from the main recharge area in the Appalachian Mountains to the St. Lawrence River (Figure 1) [Larocque et al., 2013]. Groundwater mainly discharges as base flows in the Becancour

River and its tributaries. Local recharge occurs in the lower part of the watershed, where Champlain Sea clays are discontinuous [Larocque *et al.*, 2013], complicating the groundwater flow path. The hydraulic conductivities of the Ordovician fractured bedrock aquifer are low to moderate ($\sim 10^{-9}$ to 10^{-6} m s $^{-1}$), while those of the Quaternary aquifer are moderate ($\sim 10^{-6}$ to 10^{-5} m s $^{-1}$). Porosities are 1–5% and 10–20%, respectively, for the Ordovician fractured aquifer and for the Quaternary granular aquifer [Tran Ngoc *et al.*, 2014; Benoît *et al.*, 2011]. Groundwater has a low salinity, of between 0.06 and 0.78 g L $^{-1}$. Groundwater types are as follows [Mezonnat *et al.*, 2016]: (1) Ca-HCO $_3$ and Ca-HCO $_3$ -SO $_4$ in freshwater near the Appalachian Foothills main recharge; (2) Na-HCO $_3$ and Na-HCO $_3$ -SO $_4$ evolved water, with Ca $^{2+}_{\text{dissolved}}$ exchanged with Na $^{+}_{\text{mineral}}$ in the middle portion of the watershed; and (3) slightly mineralized waters (Ca-HCO $_3$ -Cl, Na and Na-HCO $_3$ -Cl types) close to the St. Lawrence River, where chlorine is derived from marine-glacial pore water originating from the Champlain Sea marine transgression.

Groundwater ages calculated with radionuclide-based methods are variable. Freshwater containing tritium has been dated at less than 60 years using the $^3\text{H}/^3\text{He}$ method [Vautour *et al.*, 2015]. More evolved waters have uncorrected ^{14}C up to 15 kyr, while NETHPATH ^{14}C -adjusted equivalent ages are up to 6.7 kyr [Vautour *et al.*, 2015]. These values are in the range of those obtained by other authors in neighboring watersheds of the St. Lawrence Lowlands, ranging from 17–6 kyr (Nicolet-St. François watershed) [Saby *et al.*, 2016] to 14–4 kyr (Monteregie Est watershed) [Beaudry, 2013].

3. Methods

3.1. Sampling and Analytical Procedures

Groundwater from the Ordovician aquifer was sampled from 20 municipal, domestic, and instrumented wells, with depths ranging between 15 and 65 m. Wells drilled into the fractured aquifer are equipped with a casing through the sections crossing the unconsolidated Quaternary deposits. They are open boreholes when they reach the Ordovician-age-fractured aquifer. Three domestic wells were sampled from the Quaternary aquifer, at depths ranging from 6 to 15 m (BEC105, BEC117, and BEC118), and all were equipped with a casing and a bottom screen. A Waterra® Inertial Pump System was used to collect water from domestic and instrumented wells. Water was collected at the wellhead in municipal pumping stations. Groundwater was collected for helium analyses using a copper tube (9.5 cm of diameter), sealed with clamps to avoid atmospheric contamination [e.g., Vautour *et al.*, 2015]. Water for uranium isotopic analyses was collected in 1 L Nalgene® bottles, filtered (0.7 μm Millipore), and acidified to a pH of ~ 2 . Helium was measured with a MAP-215 mass spectrometer at the University of Michigan. Please refer to Castro *et al.* [2009] and Vautour *et al.* [2015] for details on the analytical procedures, uncertainties, and reproducibility of helium isotopic analyses. Uranium was extracted using a method modified from Edwards *et al.* [1987] and analyzed with a VG-SECTOR Thermo-Ionization Mass Spectrometer equipped with an ion counter at the radioisotope laboratory of GEOTOP in Montréal. Analytical uncertainties on U concentrations were less than 1%. Uncertainties on the $(^{234}\text{U}/^{238}\text{U})_{\text{act}}$ vary from 0.4 to 5%, with an average error of $\sim 1.3\%$ (2σ). Please refer to Méjean *et al.* [2016] for details on U isotopic analyses.

3.2. Modeling ^{234}U Release Into Groundwater

To quantify the release of both radiogenic ^4He and ^{234}U isotopes into groundwater, a coupled model of ^{234}U - ^{238}U fractionation and ^4He enhanced accumulation rate was developed using relevant equations from Andrews *et al.* [1982] and Solomon *et al.* [1996].

The ejection and accumulation rates of ^{234}U in groundwater were simulated using the relationship between stress-induced fracturing of the aquifer matrix and the formation of new exchange surfaces where α -recoil can preferentially take place, facilitating the release of ^{234}U [Andrews *et al.*, 1982]. This model assumes that groundwater acquires U by partial dissolution of rock at the recharge site and may undergo evolution in its uranium concentration by water-rock interaction, or after U deposition by ejection of ^{234}U caused by ^{234}Th recoil.

For groundwater in a reducing environment with an initial $(^{234}\text{U}/^{238}\text{U})_{\text{initial,act}}$ entering the α -recoil zone (i.e., an aquifer under reducing conditions where α -recoil dominated over dissolution), the evolution of the activity ratio with the age of the groundwater $(^{234}\text{U}/^{238}\text{U})_{\text{act,final}}$ can be estimated using the following relationship of Andrews *et al.* [1982]:

$$\left(\frac{^{234}\text{U}}{^{238}\text{U}}\right)_{\text{act,final}} = 1 + \left[\left(\frac{^{234}\text{U}}{^{238}\text{U}}\right)_{\text{act,initial}} - 1\right] \times e^{(-^{234}\lambda t)} + 0.235 \times \rho \times S \times R \times \left[1 - e^{(-^{234}\lambda t)}\right] \times \frac{[U]_{\text{rock}}}{[U]_{\text{water}}} \quad (1)$$

In equation (1), the first term accounts for the decay of the ^{234}U excess accumulated in groundwater during recharge (i.e., in the unconfined part of the aquifer). The second term accounts for the α -recoil effect on the $(^{234}\text{U}/^{238}\text{U})_{\text{act}}$ when groundwater reaches the confined part of the aquifer (i.e., under reducing conditions) [Andrews *et al.*, 1982]. The variable S is the specific surface area (i.e., the surface area of rock in contact with water (in $\text{cm}^2 \text{cm}^{-3}$)); ρ is the density of the aquifer rock (2.72 g cm^{-3} for the carbonate-dominated lithologies found in the Becancour aquifers); 0.235 is the probability that ^{234}Th atoms actually escape from the rock surface into the water [Bonotto and Andrews, 1993]; $^{234}\lambda$ is the ^{234}U decay constant ($2.826 \times 10^{-6} \text{ yr}^{-1}$) [Cheng *et al.*, 2000]; $[U]_{\text{rock}}$ and $[U]_{\text{water}}$ are the U content in the aquifer rock and in the water, respectively; and R is the distance of α -recoil for ^{234}Th , which is estimated to be $3 \times 10^{-6} \text{ cm}$ in Andrews and Kay [1983].

The boundary conditions for the model are (1) $(^{234}\text{U}/^{238}\text{U})_{\text{act,final}}$ depends on $(^{234}\text{U}/^{238}\text{U})_{\text{act,initial}}$ at $t = 0$, and corresponds to the activity ratio recorded in the water when entering the α -recoil-dominated zone, which corresponds to the shallowest groundwater sampled in the study area (BEC118; $(^{234}\text{U}/^{238}\text{U})_{\text{act}} = 1.14$) [Méjean *et al.*, 2016]; (2) $[U]_{\text{rock}}$ is the mean value (1.14 ppm) measured by Vautour *et al.* [2015] in aquifer rock samples and $[U]_{\text{water}}$ is the mean uranium concentration (0.04 ppb) measured in groundwater samples from the semiconfined and confined parts of the aquifer ($n = 7$) [Méjean *et al.*, 2016]; and (3) t is the groundwater residence time. In the simulation, the S ($\text{cm}^2 \text{cm}^{-3}$) necessary to obtain a $(^{234}\text{U}/^{238}\text{U})_{\text{act}}$ of 6.07 in the BEC101 6.7 kyr-old groundwater was calculated, extrapolating it from equation (1) as follows:

$$S = \frac{\left(\frac{^{234}\text{U}}{^{238}\text{U}}\right)_{\text{act,final}} - \left[\left(\frac{^{234}\text{U}}{^{238}\text{U}}\right)_{\text{act,initial}} - 1\right] \times e^{(-^{234}\lambda t)}}{0.235 \times \rho \times R \times \left(1 - e^{(-^{234}\lambda t)}\right)} \quad (2)$$

From S , and assuming an aquifer matrix composed of grains produced by stress-induced fracturing, the grain size, r (cm), is deduced from the relationship of Bonotto and Andrews [1993]:

$$r = \frac{3}{\phi \times S} \quad (3)$$

In equation (3), the term ϕ is the mean matrix porosity, which is assumed to be 3% for the Becancour fractured aquifer [Vautour *et al.*, 2015].

3.3. Modeling ^4He Release Into Groundwater

The ^4He release model of Solomon *et al.* [1996] assumes helium diffusion out of a spherical grain. The diffusive flux of radiogenic ^4He from a single grain is calculated using Fick's first law of diffusion. The equation that governs the release of helium per unit of weight of solids, N ($\text{cm}^3 \text{STP g}_{\text{rock}}^{-1}$), is [Solomon *et al.*, 1996]

$$N = 6 \times \lambda \times (C_0 - C_w K_{ws}) \times \Sigma e^{(-\lambda n^2 \pi^2 t)} \quad (4)$$

where λ (s^{-1}) is the leakage coefficient that determines the rate at which previously accumulated He diffuses from the aquifer solids into groundwater; n is the number of sequences generated using the iterative method; C_0 is the initial concentration in the grain; C_w is the ^4He concentration measured in the groundwater; and K_{ws} is the partition coefficient for He in a water-solid system, assumed to be 1 [Solomon *et al.*, 1996].

The leakage coefficient, λ , depends in turn on the grain size of the aquifer matrix, through the relationship:

$$\lambda = \frac{D_s}{r^2} \quad (5)$$

where D_s is the solid-state diffusion coefficient (i.e., diffusion initiated in the solid phase by the occurrence of surface defects, which include grain boundaries; $\text{cm}^2 \text{ s}^{-1}$), and r is the geometric mean grain size (cm).

4. Results and Discussion

4.1. U-Th Isotope Systematics in Groundwater of the Becancour Aquifer

The measured uranium concentrations in the Becancour fractured aquifer of Ordovician age are very low and display a high degree of variability, with values ranging from 0.003 ± 0.00002 to 2.939 ± 0.012 ppb

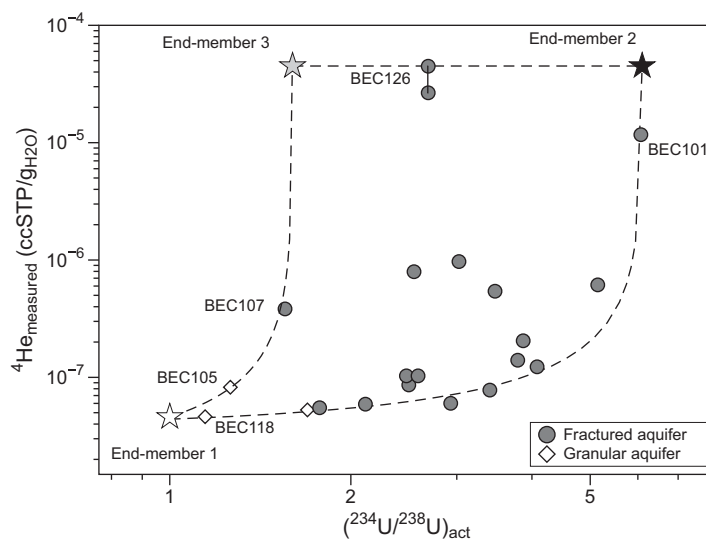


Figure 2. ^4He concentrations in groundwater plotted against the $(^{234}\text{U}/^{238}\text{U})_{\text{act}}$ measured in the Becancour fractured (gray circles) and granular (white diamonds) aquifers. Groundwater end-members (stars) and mixing curves (dashed lines) are also indicated. See text for details.

Water (ASW; $4.6 \times 10^{-8} \text{ cm}^3 \text{ STP g}_{\text{H}_2\text{O}}^{-1}$ at 10°C) [Smith and Kennedy, 1983]. The $(^{234}\text{U}/^{238}\text{U})_{\text{act}}$ should be close to unity (i.e., at secular equilibrium). Indeed, freshwater in the area is of Ca- HCO_3 type and derives from the dissolution of carbonates in the unconfined part of the aquifer. Dissolution of the rock is a zero-order rate process that results in the transfer of U into groundwater with the same $(^{234}\text{U}/^{238}\text{U})_{\text{act}}$ as the bulk rock, which is closer to the secular equilibrium [Méjean et al., 2016]. Freshwater of well BEC118 best represents this end-member, with $^4\text{He} = 6.04 \times 10^{-8} \text{ cm}^3 \text{ STP g}_{\text{H}_2\text{O}}^{-1}$ and $(^{234}\text{U}/^{238}\text{U})_{\text{act}} = 1.14$ [Méjean et al., 2016]. The $^3\text{H}/^3\text{He}$ calculated age for this sample is 2.7 ± 0.1 years [Vautour et al., 2015]. The second component is older groundwater, having accumulated large amounts of radiogenic ^4He ($1.2\text{--}4.5 \times 10^{-5} \text{ cm}^3 \text{ STP g}_{\text{H}_2\text{O}}^{-1}$) and showing the most fractionated $(^{234}\text{U}/^{238}\text{U})_{\text{act}}$ value, of up to 6 (end member 2; black star; Figure 2). This evolved water was identified with that collected at well BEC101. Interestingly, this groundwater has a Na- HCO_3 chemistry, indicating longer water-rock interaction by ionic exchange [Mezonnat et al., 2016]. This groundwater was sampled in the confined part of the fractured bedrock, where dissolution processes are negligible, and where $^{234}\text{U}\text{--}^{238}\text{U}$ fractionation is dominated by α -recoil processes [Méjean et al., 2016]. The uncorrected ^{14}C age of BEC101 groundwater is 15.4 kyr and the NETPATH ^{14}C -adjusted age is 6.7 kyr.

Most of the samples plot on a mixing line connecting end-members 1 and 2 (Figure 2). To explain the scattered points that do not lie on the mixing curve between end-members 1 and 2, a third end-member is required. Two samples (BEC105 and BEC107) plot on a mixing line between end-member 1 and a third end-member containing large amounts of radiogenic ^4He ($1.2\text{--}4.5 \times 10^{-5} \text{ cm}^3 \text{ STP g}_{\text{H}_2\text{O}}^{-1}$), but only slightly fractionated, with $(^{234}\text{U}/^{238}\text{U})_{\text{act}}$ of up to 1.6. Groundwater sampled from well BEC126 derives from the mixing of end-members 3 and 2 (Figure 2). BEC126 is an important, yet intriguing sample. The well is located upgradient, closer to the recharge area. Groundwater, of Ca- HCO_3 type, is the least saline in the Becancour River watershed, with a Total Dissolved Solids (TDS) concentration of 0.22 g L^{-1} [Vautour et al., 2015]. Even if the highest ^4He content in the watershed was measured in BEC126 ($4.5 \times 10^{-5} \text{ cm}^3 \text{ STP g}_{\text{H}_2\text{O}}^{-1}$) [Vautour et al., 2015], the water chemistry and the occurrence of a notable amount of tritium (4.4 TU) clearly indicates that freshwater dominates. To resolve this apparent contradiction (i.e., freshwater containing large excesses of radiogenic ^4He), it must be assumed that this sample represents the situation where rock dissolution liberates the ^4He that was produced, partially retained and accumulated in the aquifer matrix for a long, geological time. The occurrence of the third end-member, enriched in radiogenic helium, would support the model of Solomon et al. [1996], which suggests that aquifer grains partially retain radiogenic ^4He for long, geological periods. Dissolution of the rock and the release of the accumulated radiogenic helium would create the observed ^4He excess in groundwater, together with a $(^{234}\text{U}/^{238}\text{U})_{\text{act}}$ of close to unity (Figure 2).

[Méjean et al., 2016]. Based on relationships between U and Cl and SO_4 contents, Méjean et al. [2016] concluded that uranium concentration in groundwater is mainly controlled by the redox condition in the aquifer.

The $(^{234}\text{U}/^{238}\text{U})_{\text{act}}$ plotted against the concentration of ^4He in groundwater from the Ordovician fractured aquifer (Figure 2) suggests that ^4He and $(^{234}\text{U}/^{238}\text{U})_{\text{act}}$ result from a three-component mixing.

The first component is freshwater from modern recharge (end member 1, white star; Figure 2). The ^4He concentration is expected to be close to that from solubility equilibrium with the atmosphere, or Air Saturated

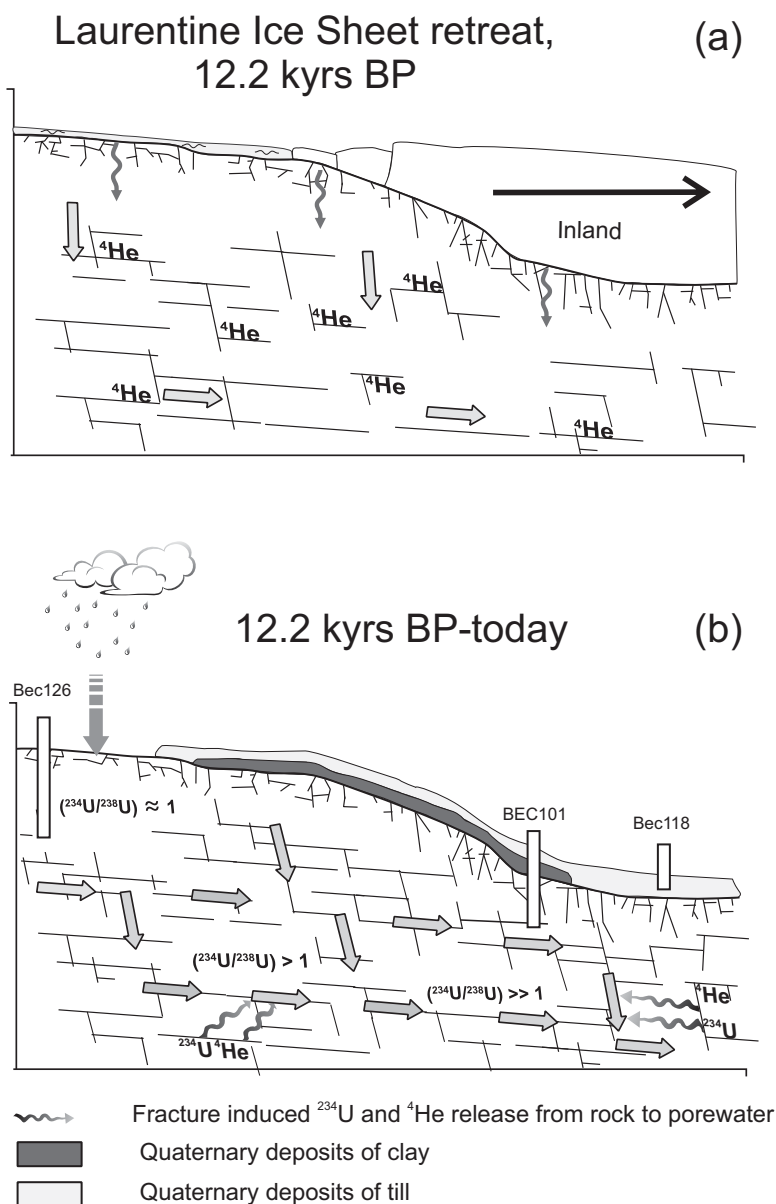


Figure 3. Schema of the Beancour watershed fractured aquifer with: condition of water circulation in the system during waning stages of the Laurentide Ice Sheet retreat (a) \sim 12.2 kyr and (b) between 12.2 kyr (initiation of deglaciation) and the present day.

4.2. Causes of Enhanced ^{234}U and ^4He Release Into Groundwater

The cause of ^4He and ^{234}U release and accumulation in groundwater is assumed here to be rock fracturing. Radiogenic ^4He is released from the rock and accumulated into groundwater through diffusion and α -recoil [Torgersen, 1980; Torgersen and O'Donnell, 1991]. If the grain size is larger than the α -recoil distance (30–100 nm for ^{234}Th ; 30–100 μm for ^4He) [Harvey, 1962] or its diffusion length ($\sqrt{D \cdot t}$), only a fraction of the radiogenic ^4He accumulated in the rock will be released into the groundwater [Solomon *et al.*, 1996]. Part of the produced radiogenic helium will instead be retained in the rock until rock fracturing either increases the grain surface area, facilitating helium release by diffusion, and/or reduces the grain size, facilitating helium ejection by α -recoil [Solomon *et al.*, 1996].

The main mechanism of ^{234}U release into groundwater is also α -recoil but is a more complex, multistep process than for helium. When ^{238}U contained in the rock decays, α -particles transmit the kinetic energy to ^{234}Th , the ^{238}U daughter nuclide. A portion of the ^{234}Th is ejected from the grain into the water. The insoluble ^{234}Th is adsorbed onto the grain surface and then decays to ^{234}U . The ^{234}U located in damaged lattice

sites or on the surface of the grain will escape into the water, while ^{238}U will mainly be retained in the crystal lattice [Kigoshi, 1971]. As is the case for helium, the larger the surface area that is exposed to water increases the probability that ^{234}U is near the grain surface, facilitating its release into pore water.

Continental ice sheets played an important role in the Quaternary hydrogeology of North America [McIntosh and Walter, 2005, 2006; Neuzil, 2012; McIntosh et al., 2011; Person et al., 2012]. The Laurentide Ice Sheet retreat, initiated around 12,200 years ago, could be the main cause of stress-induced changes and associated mechanical fracturing of the Becancour bedrock aquifer (Figure 3). Loading and unloading caused by the Laurentide Ice Sheet migration might have induced large-scale near-surface tectonic stresses, inducing subvertical tensile fractures used by groundwater as flow paths [Lemieux et al., 2008].

As the Laurentide Ice Sheet started to retreat, large amounts of subglacial water flowed in the aquifer, promoting the partial dissolution of the aquifer rocks. This process is expected to have released U with little ^{234}U - ^{238}U isotopic fractionation ($(^{234}\text{U}/^{238}\text{U})_{\text{act}} \approx 1$) (Figure 3a). Bedrock dissolution also caused the rapid release of large amounts of ^4He accumulated over time in the bedrock into the water (Figure 3a). This situation might reflect the U-He isotopic composition of end-member 3 in Figure 2. If sample BEC126 contains this meltwater (Figure 2), then it should be imprinted in its isotopic signature. The stable isotopic composition of BEC126 groundwater shows a $\delta^{18}\text{O}$ value of -11.7‰ , which is heavier than the expected $\delta^{18}\text{O}$ value of -16.5‰ for glacial meltwater in the area [Cloutier et al., 2010; Montcoudiol et al., 2015]. However, the noble gas calculated paleotemperature (NGT) [Stute and Schlosser, 1993] for BEC126 is $-0.26 \pm 3^\circ\text{C}$, significantly colder ($3\text{--}7^\circ\text{C}$) than the other water samples in the region [Vautour et al., 2015].

Between 12.2 and 6.7 kyr before present, the near-surface stress induced by the ice sheet retreat increased fracture density as isostatic rebound and unbending of the crust progressed [Grollmund and Zoback, 2000; Lamarche et al., 2007] (Figure 3b). Over the past 6.7 kyr, the hydrogeological system of the St. Lawrence Platform reached the present-day configuration (Figure 3b). The invasion of subglacial water ended, and newly recharged water started to flow into a more highly fractured aquifer and to accumulate ^{234}U and ^4He released through the newly formed surfaces in the reduced and confined part of the aquifer. This situation is illustrated by fractionated $(^{234}\text{U}/^{238}\text{U})_{\text{act}}$ ratios of up to 6.07, accompanied by large amounts of radiogenic ^4He , as observed in the 6.7 kyr-old BEC101 groundwater (end-member 2 in Figure 2).

4.3. Modeling the Release of ^{234}U and ^4He Into Groundwater

Once groundwater reaches reducing conditions in the aquifer, and the chemical leaching of ^{234}U ceases, $(^{234}\text{U}/^{238}\text{U})_{\text{act}}$ may evolve over time to a balance between the ^{234}U physical leaching and its decay. The $(^{234}\text{U}/^{238}\text{U})_{\text{act}}$ evolution can be seen in Figure 4, where $(^{234}\text{U}/^{238}\text{U})_{\text{act}}$ is plotted against groundwater residence time. The simulation is done using equation (1), and was calculated using an initial $(^{234}\text{U}/^{238}\text{U})_{\text{act}}$ of 1.14 (BEC118; representing the activity ratio recorded in the water before entering the confined part of the aquifer) and a final $(^{234}\text{U}/^{238}\text{U})_{\text{act}}$ value of 6.07 (BEC101; the maximum value measured in groundwater from the

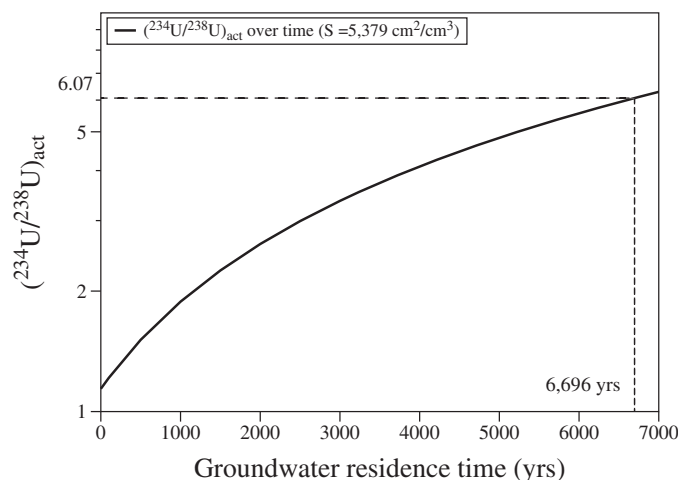


Figure 4. Simulated $(^{234}\text{U}/^{238}\text{U})_{\text{act}}$ evolution as a function of groundwater residence time, calculated with equation (1) and using a surface area, S , of $5379\text{ cm}^2\text{ cm}^{-3}$.

deeper Ordovician aquifer), after a contact time of 6.7 kyr, the ^{14}C -adjusted age for BEC101 groundwater [Vautour et al., 2015]. Using the relationship described above and equation (2), an S of $5379\text{ cm}^2\text{ cm}^{-3}$ is calculated. This specific surface represents the extent of rock surface in contact with pore water.

The relationship between specific surface and grain size (equation (3)) is used to calculate a grain radius of $18\text{ }\mu\text{m}$. The calculated grain size is even lower than the recoil path length of an alpha particle [Torgersen and Stute, 2013]. This means that the produced radiogenic ^4He will not be retained in

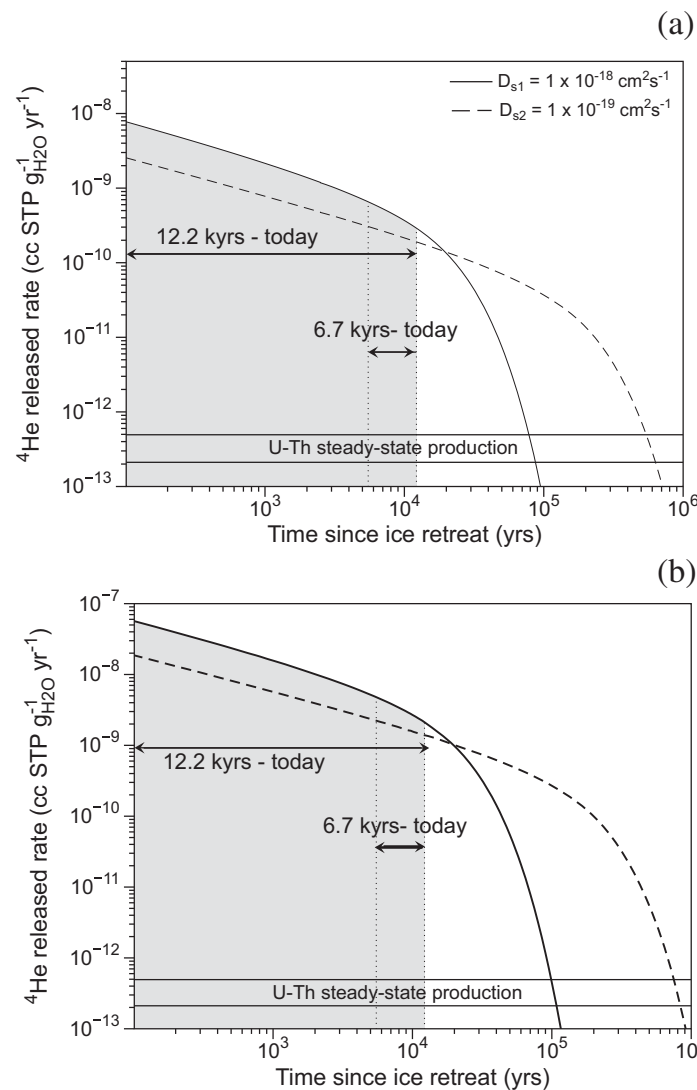


Figure 5. ^4He release rates into groundwater as a function of time since ice retreat (12.2 kyr ago) and of time of BEC101 (6.7 kyr), simulated using equation (4). The solid line represents the simulation for a diffusion coefficient of $D_{s1} = 1 \times 10^{-18} \text{ cm}^2 \text{ s}^{-1}$, and the dashed line for a diffusion coefficient $D_{s2} = 1 \times 10^{-19} \text{ cm}^2 \text{ s}^{-1}$. Figures show simulations with a remaining amount of helium preserved in the aquifer grain of (a) $C_0=27\%$ and (b) $C_0=90\%$.

and D_s , the helium diffusion coefficient (in $\text{cm}^2 \text{ s}^{-1}$), are the most difficult parameters to constrain but are essential.

Assuming an average ^4He production rate of $3.5 \pm 1.4 \times 10^{-13} \text{ cm}^3 \text{ STP g}_{\text{rock}}^{-1} \text{ yr}^{-1}$, calculated using U and Th contents measured in the aquifer rocks by [Vautour *et al.*, 2015], and an average formation age of 445 Ma, the total amount of ^4He produced is $1.6 \pm 0.9 \times 10^{-4} \text{ cm}^3 \text{ STP g}_{\text{rock}}^{-1}$. This amount cannot be taken directly as C_0 , because helium is continuously diffused out the aquifer grains, also at ambient temperature [e.g., Mamyrin and Tolstikhin, 1984]. To calculate the remaining amount of helium preserved in the aquifer grains, the steady state release factor of helium, $\Lambda_{4\text{He}}$ ($^4\text{He}_{\text{released}}/^4\text{He}_{\text{produced}}$) [e.g., Torgersen, 1980; Torgersen and Stute, 2013] also needs to be calculated. This can theoretically be calculated using equations based on α -recoil, rapid or slow diffusion, or weathering, which are the three main helium release mechanisms suggested by Torgersen [1980]. However, an accurate estimate of $\Lambda_{4\text{He}}$ requires precise knowledge of the grain size, prior to glacial-induced fracturing, which is not the case for the current study. There is an alternative approach to estimate the $\Lambda_{4\text{He}}$. Vautour *et al.* [2015] noted that the calculated U-Th/ ^4He ages for samples BEC112, 137, 138, 147, and 148 were much lower (250–1808 years) than the ^{14}C ages (3288–7342

the grain and should be released by α -recoil and diffusion from the grain, and thus provided a local ^4He input into the aquifer.

Using only one S value for the entire regional aquifer is a major limitation of our model. It is known that there is older groundwater in the region, with corrected ^{14}C ages of higher than 10 kyr [Saby *et al.*, 2016], but the $(^{234}\text{U}/^{238}\text{U})_{\text{act}}$ was not measured. If we assume that the maximum $(^{234}\text{U}/^{238}\text{U})_{\text{act}}$ value in the region is 6.07, then the maximum grain size associated with, e.g., 12.2 kyr-old groundwater (equivalent to the time since deglaciation began) will be $33 \mu\text{m}$. Further U isotope measurements in old groundwater samples are needed to obtain a reasonable average value for the surface area and thus for the aquifer grain size.

The calculated grain size radius of $18 \mu\text{m}$ is used to estimate the release of helium per unit weight of solids, N (in $\text{cm}^3 \text{ STP g}_{\text{rock}}^{-1} \text{ yr}^{-1}$), since the start of the last deglaciation ($t_0 = 12.2 \text{ ka}$), using equation (4) [Solomon *et al.*, 1996]. Results of the simulation are reported in Figure 5. In equation (4), C_0 , the amount of radiogenic ^4He (in $\text{cm}^3 \text{ STP g}_{\text{rock}}^{-1}$) produced and retained in the grain since its deposition

years). To explain this discrepancy, it is either assumed that the radiogenic He production rate is much lower than the average value of $3.5 \pm 1.4 \times 10^{-13} \text{ cm}^3 \text{ STP g}_{\text{rock}}^{-1} \text{ yr}^{-1}$ or that radiogenic helium is partially retained in the rock, with a calculated $\Lambda_{4\text{He}}$ ranging from 0.07 to 0.27. Assuming that the calculated $\Lambda_{4\text{He}}$ are typical steady state release factors of the studied aquifers and that they did not substantially change over time, C_0 in equation (4) can be calculated to be $1.04 \pm 0.7 \times 10^{-4} \text{ cm}^3 \text{ STP g}_{\text{rock}}^{-1}$, corresponding to a helium loss of 27% of the total accumulated amount ($C_0 - 27\% = C_{01}$). This value can be considered to be a very conservative upper limit. The lower limit can reasonably assumed to be 10% of the total produced radiogenic helium. The calculated lower initial concentration is $1.6 \pm 0.9 \times 10^{-5} \text{ cm}^3 \text{ STP g}_{\text{rock}}^{-1}$ ($C_0 - 90\% = C_{02}$).

The second parameter to estimate is the diffusion coefficient of He, which can vary greatly pending the mineral phase and lithology of where it resides. In the present work, two values of the diffusion coefficient, D_{s1} , are assumed for the carbonate-rich shale dominant lithology of the regional fractured aquifer: $D_{s1} = 1.0 \times 10^{-18} \text{ cm}^2 \text{ s}^{-1}$ and $D_{s2} = 1.0 \times 10^{-19} \text{ cm}^2 \text{ s}^{-1}$. These values encompass the range of diffusion coefficients obtained for carbonate [Copeland et al., 2007; Pinti et al., 2012] and silicate rocks [Solomon et al., 1996]. It is worth noting that laboratory experiments are needed in the near future to measure the helium diffusion coefficient in the aquifer matrix, as done previously in similar studies [Solomon et al., 1996; Carey et al., 2004].

Figure 5 reports the results of the simulated radiogenic helium release rate since the last deglaciation, assuming a $C_{01} = 1.04 \pm 0.7 \times 10^{-4} \text{ cm}^3 \text{ STP g}_{\text{rock}}^{-1}$ (Figure 5a) and a $C_{02} = 1.6 \pm 0.9 \times 10^{-5} \text{ cm}^3 \text{ STP g}_{\text{rock}}^{-1}$ (Figure 5b) respectively. In each diagram, the two curves have been calculated for the two diffusion coefficients D_{s1} and D_{s2} , respectively.

In these simulations, it can be observed that between 100,000 years (using C_{01} ; Figure 5a) and 90,000 years (using C_{02} , Figure 5b) are required before the high helium release rate induced by fracturing reached the steady state production in the rock (i.e., $3.5 \pm 1.4 \times 10^{-13} \text{ cm}^3 \text{ STP g}_{\text{rock}}^{-1} \text{ yr}^{-1}$). By integrating the release rate of helium, N, for the time the water was in contact with the fractured aquifer (i.e., its residence time in years), the total amount of radiogenic ^4He released into groundwater is obtained. For these simulations, a minimum residence time of 6.7 kyr has been assumed, based on the adjusted ^{14}C age of BEC101 [Vautour et al., 2015]. The maximum residence time has been taken as equal to 12.2 kyr, the age of deglaciation in the region. As noted by several studies in this region [Cloutier et al., 2006; Beaudry, 2013; Saby et al., 2016], the maximum water residence time in the St. Lawrence Lowlands coincides with the Laurentide Ice Sheet retreat. This postglaciated groundwater contains large amounts of radiogenic ^4He , equivalent to that measured in BEC101, as also noted by Saby et al. [2016].

Assuming an initial ^4He concentration in the rock, prior to fracturing, of $C_{01} = 1.04 \pm 0.7 \times 10^{-4} \text{ cm}^3 \text{ STP g}_{\text{rock}}^{-1}$, the total amount of ^4He accumulated in groundwater will range from $2.85 \times 10^{-5} \text{ cm}^3 \text{ STP g}_{\text{rock}}^{-1}$ ($t_0 = 6.7 \text{ kyr}$ and $D_{s2} = 1.0 \times 10^{-19} \text{ cm}^2 \text{ s}^{-1}$) to $8.97 \times 10^{-5} \text{ cm}^3 \text{ STP g}_{\text{rock}}^{-1}$ ($t_0 = 12.2 \text{ kyr}$ and $D_{s1} = 1.0 \times 10^{-18} \text{ cm}^2 \text{ s}^{-1}$). Assuming an initial ^4He concentration in the rock of $C_{02} = 1.6 \pm 0.9 \times 10^{-5} \text{ cm}^3 \text{ STP g}_{\text{rock}}^{-1}$, the total amount of ^4He accumulated in groundwater will range from $3.89 \times 10^{-6} \text{ cm}^3 \text{ STP g}_{\text{rock}}^{-1}$ ($t_0 = 6.7 \text{ kyr}$ and $D_{s2} = 1.0 \times 10^{-19} \text{ cm}^2 \text{ s}^{-1}$) to $1.22 \times 10^{-5} \text{ cm}^3 \text{ STP g}_{\text{rock}}^{-1}$ ($t_0 = 12.2 \text{ kyr}$ and $D_{s1} = 1.0 \times 10^{-18} \text{ cm}^2 \text{ s}^{-1}$). Except for the ^4He concentration calculated using the lower C_{02} , a residence time of 6.7 kyr, and the slowest diffusion coefficient, D_{s2} , all other simulated helium concentrations are within the range of concentrations previously measured in St. Lawrence Lowlands groundwater, from $1.16 \times 10^{-5} \text{ cm}^3 \text{ STP g}_{\text{H}_2\text{O}}^{-1}$ to $7.75 \times 10^{-5} \text{ cm}^3 \text{ STP g}_{\text{H}_2\text{O}}^{-1}$ [Pinti et al., 2013; Vautour et al., 2015; Saby et al., 2016]. An important implication of the spherical diffusion model is that the fractured aquifer will release ^4He at a higher rate over thousands of years than will the steady state U-Th ^4He production. It can be assumed that ^4He released since deglaciation could explain radiogenic ^4He currently measured in the aquifer if ^4He loss through the top of the aquifer is limited.

4.4 Implications for Calculating (U-Th)/ ^4He Groundwater Ages

Assuming that radiogenic ^4He measured in groundwater is mainly produced locally by U and Th decay, (U-Th)/ ^4He groundwater residence times can be estimated following the relationship:

$$t = \frac{[{}^4\text{He}_{\text{terr}}]}{P_{4\text{He}} \times \Lambda_{4\text{He}} \times \left(\frac{1-\phi}{\phi}\right) \times \rho} \quad (6)$$

$[{}^4\text{He}_{\text{terr}}]$ is the amount of radiogenic ^4He measured in groundwater ($\text{cm}^3 \text{ STP g}_{\text{water}}^{-1}$); $P_{4\text{He}}$ is the radiogenic ^4He production rate by U and Th decay ($\text{cm}^3 \text{ STP g}_{\text{rock}}^{-1} \text{ yr}^{-1}$); $\Lambda_{4\text{He}}$ is the He retention factor

(${}^4\text{He}_{\text{released}}/{}^4\text{He}_{\text{produced}}$) (i.e., the fraction of He produced in the grain and released into the pore water); $(1 - \phi/\rho)$ is the void ratio, with ϕ being the porosity; and ρ is the density of the aquifer matrix.

The most difficult parameter to estimate is the He retention factor, $\Lambda_{4\text{He}}$, because of the various mechanisms by which ${}^4\text{He}$ is transferred from the grain to the water: α -recoil, diffusion through mineral defects, bulk dissolution, or weathering [Torgersen, 1980]. A release factor, $\Lambda_{4\text{He}}$, of 1 is an approximation largely used in groundwater studies [Torgersen and Stute, 2013], because grain size is generally on the same order of magnitude as the recoil distance range. As described above, fracturing following ice sheet retreat dramatically reduced the grain diameter, exposing the accumulated ${}^4\text{He}$, which was then released into pore water. Therefore, the release factor, $\Lambda_{4\text{He}}$, should be greater than 1. Solomon *et al.* [1996] calculated helium release rates of $1.3\text{--}2.3 \times 10^{-10} \text{ cm}^3 \text{ STP g}^{-1} \text{ yr}^{-1}$ in Sturgeon Falls, Ontario, Canada. Such release rates ($\Lambda_{4\text{He}}$ on the order of 300–600) were confirmed by laboratory measurements of the diffusion coefficient for quartz grains [Solomon *et al.*, 1996]. Helium release rates calculated here for the Ordovician fractured aquifer range from 4.2 to $106 \times 10^{-10} \text{ cm}^3 \text{ STP g}^{-1} \text{ yr}^{-1}$ (i.e., 2–46 times those calculated in Sturgeon Falls by Solomon *et al.* [1996]). The resulting $\Lambda_{4\text{He}}$ is in the range of 10^3 to 10^4 . The difference between $\Lambda_{4\text{He}}$ calculated by Solomon *et al.* [1996] and those from this study might be related to the choice of the helium diffusion coefficients used, which are unknown for the carbonate-rich shale lithology of the St. Lawrence Lowlands aquifers. Helium release rates and diffusion coefficients must therefore be determined through laboratory experiments in order to correctly estimate the He retention factor, and thus (U-Th)/ ${}^4\text{He}$ groundwater ages.

4. Conclusions

In the present work, the sources of radiogenic ${}^4\text{He}$ in groundwater from the fractured regional aquifer of the St. Lawrence Lowlands were reevaluated. The relationship between U fractionation and radiogenic ${}^4\text{He}$ excesses suggests a process within the aquifer to explain the ${}^{234}\text{U}$ and ${}^4\text{He}$ excesses, providing a complementary approach to the hypothesis previously suggested by Vautour *et al.* [2015] of external sources of helium. Using a coupled model of ${}^{234}\text{U}$ and ${}^4\text{He}$ release from aquifer grains following glacial-induced rock fracturing, it has been shown that the instantaneous release of accumulated helium from the host rock could be between 4.2×10^{-10} and $1.06 \times 10^{-8} \text{ cm}^3 \text{ STP g}_{\text{H}_2\text{O}}^{-1} \text{ yr}^{-1}$. These values are 10^3 to 10^4 times higher than the annual steady state production from U and Th decay, of $3.5 \pm 1.4 \times 10^{-13} \text{ cm}^3 \text{ STP g}_{\text{H}_2\text{O}}^{-1} \text{ yr}^{-1}$.

The results of this work do not preclude the existence of an external ${}^4\text{He}$ flux resulting from He production within the crystalline basement beneath the studied sedimentary basin and entering the bottom of the aquifers. However, as noted by Torgersen and Stute [2013], glacial-produced fracturing and the related enhanced release of ${}^4\text{He}$ ($\Lambda_{4\text{He}} \gg 1$) may be common at high latitudes and may provide a dominant ${}^4\text{He}$ input within periglacial aquifer systems. The next step would be to investigate whether similar relationships between ${}^{234}\text{U}$ – ${}^{238}\text{U}$ fractionation and helium isotopes exist in other hydrological systems and in different climates, suggesting either internal sources of helium in groundwater generally or that enhanced ${}^{234}\text{U}$ and ${}^4\text{He}$ release is restricted to high-latitude aquifers.

Acknowledgments

The Ministère du Développement durable, de l'Environnement, des Parcs et de la Lutte contre les changements climatiques, Fonds de recherche du Québec - Nature et Technologies (grant 136990 to D.L.P.), Natural Sciences and Engineering Research Council of Canada (discovery grants RGPIN-2015-05378 to D.L.P. and RGPIN-2015-06744 to M.L.), Organisme de bassin versant GROBEC, Conseil régional des élus Centre-du-Québec, MRC d'Arthabaska, MRC de Bécancour, MRC de l'Érable, MRC de Nicolet-Yamaska, AGTCQ, and Cégep Thetford contributed funding to this research. The data associated with this article can be found in Méjean *et al.* [2016], <https://doi.org/10.1016/j.apgeochem.2015.12.015>. Supplementary results can be requested from the author (mejeanpauline@gmail.com).

References

- Aggarwal, P. K., *et al.* (2015), Continental degassing of ${}^4\text{He}$ by surficial discharge of deep groundwater, *Nat. Geosci.*, 8(1), 35–39.
- Andrews, J. N., and R. L. F. Kay (1983), The U contents and ${}^{234}\text{U}/{}^{238}\text{U}$ activity ratios of dissolved uranium in groundwaters from some Triassic Sandstones in England, *Chem. Geol.*, 41(1–3), 101–117.
- Andrews, J. N., I. S. Giles, R. L. F. Kay, D. J. Lee, J. K. Osmond, J. B. Cowart, P. Fritz, J. F. Barker, and J. Gale (1982), Radioelements, radiogenic helium and age relationships for groundwaters from the granites at Stripa, Sweden, *Geochim. Cosmochim. Acta*, 46(9), 1533–1543.
- Aravena, R., L. I. Wassenaar, and L. N. Plummer (1995), Estimating ${}^{14}\text{C}$ groundwater ages in a methanogenic aquifer, *Water Resour. Res.*, 31(9), 2307–2317.
- Beaudry, C. (2013), Hydrogéochimie de l'aquifère rocheux régional en Montérégie est, Québec, MS thesis, Inst. Natl. de la Rech. Sci., Québec, Canada.
- Benoit, N., D. Blanchette, M. Nastev, V. Cloutier, D. Marcotte, M. Brun Kone and J. Molson (2011), Groundwater geochemistry of the lower Chaudière river watershed, QuébecGeoHydro2011, Joint IAH-CNC, CANQUA and AHQ Conference, August 28–31, 2011, Paper DOC-2209 (2011), 8 pp., Québec City, Canada.
- Bonotto, D. M., and J. Andrews (1993), The mechanism of ${}^{234}\text{U}/{}^{238}\text{U}$ activity ratio enhancement in karstic limestone groundwater, *Chem. Geol.*, 103(1), 193–206.
- Bottomley, D. J., J. D. Ross, and W. B. Clarke (1984), Helium and neon isotope geochemistry of some ground waters from the Canadian Precambrian Shield, *Geochim. Cosmochim. Acta*, 48(10), 1973–1985.
- Carey, A. E., C. B. Dowling, R. J. Poreda (2004), Alabama Gulf Coast groundwaters: ${}^4\text{He}$ and ${}^{14}\text{C}$ as groundwater-dating tools, *Geology*, 32(4), 289–292.

- Castro, M. C., L. Ma, and C. M. Hall (2009), A primordial, solar He-Ne signature in crustal fluids of a stable continental region, *Earth Planet. Sci. Lett.*, *279*, 174–184.
- Cheng, H., R. L. Edwards, J. Hoff, C. D. Gallup, D. A. Richards, and Y. Asmerom (2000), The half-lives of uranium-234 and thorium-230, *Chem. Geol.*, *169*(1–2), 17–33.
- Cloutier, V., R. Lefebvre, M. M. Savard, E. Bourque, and R. Therrien (2006), Hydrogeochemistry and groundwater origin of the Basses-Laurentides sedimentary rock aquifer system, St. Lawrence Lowlands, Quebec, Canada, *Hydrogeol. J.*, *14*(4), 573–590.
- Cloutier, V., R. Lefebvre, M. M. Savard, and R. Therrien (2010), Desalination of a sedimentary rock aquifer system invaded by Pleistocene Champlain Sea water and processes controlling groundwater geochemistry, *Environ. Earth Sci.*, *59*(5), 977–994.
- Copeland, P., E. B. Watson, S. C. Urizar, D. Patterson, and T. J. Lapen (2007), Alpha thermochronology of carbonates, *Geochim. Cosmochim. Acta*, *71*(18), 4488–4511.
- Edwards, R. L., J. H. Chen, and G. J. Wasserburg (1987), U-238, U-234, Th-230, Th-232 systematics and the precise measurement of time over the past 500,000 years, *Earth Planet. Sci. Lett.*, *81*, 175–192.
- Fontes, J. C. (1992), Chemical and isotopic constraints on ¹⁴C dating of groundwater, in *Radiocarbon After Four Decades: An Interdisciplinary Perspective*, edited by R. E. Taylor et al., pp. 242–261, Springer Sci. + Bus. Media, New York.
- Gleeson, T., K. M. Befus, S. Jasechko, E. Luijendijk, and M. B. Cardenas (2016), The global volume and distribution of modern groundwater, *Nat. Geosci.*, *9*(2), 161–167.
- Godbout, P.-M. (2013), Géologie du Quaternaire et hydrostratigraphie des dépôts meubles du bassin versant de la rivière Bécancour et des zones avoisinantes, Québec, MSc thesis, Univ. du Qué. à Montréal, Montréal, Canada.
- Grollimund, B., and M. B. Zoback (2000), Post glacial lithospheric flexure and induced stresses and pore pressure changes in the northern North Sea, *Tectonophysics*, *327*(1–2), 61–81.
- Harvey, B. G. (1962), *Introduction to Nuclear Physics and Chemistry*, 382 pp., Prentice Hall, N. J.
- Holland, G., B. S. Lollar, L. Li, G. Lacrampe-Couloume, G. Slater, and C. Ballentine (2013), Deep fracture fluids isolated in the crust since the Precambrian era, *Nature*, *497*(7449), 357–360.
- Kigoshi, K. (1971), Alpha-recoil thorium-234: Dissolution into water and the uranium-234/uranium-238 disequilibrium in nature, *Science*, *173*(3991), 47–48.
- Kulongoski, J. T., and D. R. Hilton (2011), Applications of groundwater helium, in *Handbook of Environmental Isotope Geochemistry, Advances in Isotope Geochemistry*, edited by M. Baskaran, pp. 285–303, Springer, Berlin.
- Lamarque, L., V. Bondue, M. J. Lemelin, M. Lamothe, and A. Roy (2007), Deciphering the Holocene evolution of the St. Lawrence River drainage system using luminescence and radiocarbon dating, *Q. Geochronol.*, *2*(1), 155–161.
- Larocque, M., S. Gagné, L. Tremblay, and G. Meyzonnat (2013), Projet de connaissance des eaux souterraines du bassin versant de la rivière Bécancour et de la MRC de Bécancour, report III, 219 pp., Minist. du Dév. durable, de l'Environ., de la Faune et des Parcs, Quebec, Canada.
- Lehmann, B. E., et al. (2003), A comparison of groundwater dating with ⁸¹Kr, ³⁶Cl and ⁴He in four wells of the Great Artesian Basin, Australia, *Earth Planet. Sci. Lett.*, *211*(3–4), 237–250.
- Lemieux, J. M., E. Sudicky, W. Peltier, and L. Tarasov (2008), Dynamics of groundwater recharge and seepage over the Canadian landscape during the Wisconsinian glaciation, *J. Geophys. Res.*, *113*, F01011, doi:10.1029/2007JF000838.
- Lippmann-Pipke, J., B. S. Lollar, S. Niedermann, N. A. Stroncik, R. Naumann, E. Van Heerden, and T. C. Onstott (2011), Neon identifies two billion year old fluid component in Kaapvaal Craton, *Chem. Geol.*, *283*(3), 287–296.
- Mamyrin, B. A., and I. N. Tolstikhin (1984), *Helium Isotopes in Nature*, Elsevier Sci., Amsterdam.
- Marine, I. (1979), The use of naturally occurring helium to estimate groundwater velocities for studies of geologic storage of radioactive waste, *Water Resour. Res.*, *15*(5), 1130–1136.
- Mazor, E. (1995), Stagnant aquifer concept. Part 1. Large-scale artesian systems—Great Artesian Basin, Australia, *J. Hydrol.*, *173*(1), 219–240.
- McIntosh, J., and L. Walter (2005), Volumetrically significant recharge of Pleistocene glacial meltwaters into epicratonic basins: Constraints imposed by solute mass balances, *Chem. Geol.*, *222*(3), 292–309.
- McIntosh, J., and L. Walter (2006), Paleowaters in Silurian-Devonian carbonate aquifers: Geochemical evolution of groundwater in the Great Lakes region since the Late Pleistocene, *Geochim. Cosmochim. Acta*, *70*(10), 2454–2479.
- McIntosh, J., G. Garven, and J. Hanor (2011), Impacts of Pleistocene glaciation on large-scale groundwater flow and salinity in the Michigan Basin, *Geofluids*, *11*(1), 18–33.
- Méjean, P., D. L. Pinti, M. Larocque, B. Ghaleb, G. Meyzonnat, and S. Gagné (2016), Processes controlling ²³⁴U and ²³⁸U isotope fractionation and helium in the groundwater of the St. Lawrence Lowlands, Quebec: The potential role of natural rock fracturing, *Appl. Geochem.*, *66*, 198–209.
- Meyzonnat, G., M. Larocque, F. Barbecot, D. L. Pinti, and S. Gagné (2016), The potential of major ion chemistry to assess groundwater vulnerability of a regional aquifer in southern Quebec (Canada), *Environ. Earth Sci.*, *75*(1), 1–12.
- Montcoudiol, N., J. Molson, J.-M. Lemieux, and V. Cloutier (2015), A conceptual model for groundwater flow and geochemical evolution in the southern Outaouais Region, Québec, Canada, *Appl. Geochem.*, *58*, 62–77.
- Neuzil, C. (2012), Hydromechanical effects of continental glaciation on groundwater systems, *Geofluids*, *12*(1), 22–37.
- Occhietti, S., H. M. Chartier, C. Hillaire-Marcel, M. Cournoyer, S. L. Cumbaa, and R. Harington (2001), Paléoenvironnements de la Mer de Champlain dans la région de Québec, entre 11 300 et 9750 BP: le site de Saint-Nicolas, *Géogr. Phys. Quat.*, *55*(1), 23–46.
- O'Nions, R. K., and E. R. Oxburgh (1983), Heat and helium in the Earth, *Nature*, *306*, 429–431.
- Person, M., D. Butler, C. W. Gable, T. Villamil, D. Wavrek, and D. Schelling (2012), Hydrodynamic stagnation zones: A new play concept for the Llanos Basin, Colombia, *AAPG Bull.*, *96*(1), 23–41.
- Phillips, F., and M. Castro (2003), Groundwater dating and residence-time measurements, *Treatise Geochem.*, *5*, 451–497.
- Pinti, D. L., and B. Marty (1998), The origin of helium in deep sedimentary aquifers and the problem of dating very old groundwaters, *Geol. Soc. London Spec. Publ.*, *144*(1), 53–68.
- Pinti, D. L., B. Marty, and J. N. Andrews (1997), Atmosphere-derived noble gas evidence for the preservation of ancient waters in sedimentary basins, *Geology*, *25*(2), 111–114.
- Pinti, D. L., C. Béland-Otis, A. Tremblay, M. C. Castro, C. M. Hall, J. S. Marcl, J. Y. Lavoie, and R. Lapointe (2011), Fossil brines preserved in the St-Lawrence Lowlands, Québec, Canada as revealed by their chemistry and noble gas isotopes, *Geochim. Cosmochim. Acta*, *75*(15), 4228–4243.
- Pinti, D. L., B. Ghaleb, Y. Sano, S. Blanchette, E. Mathouchah, and N. Takahata (2012), Testing the U-Th/⁴He dating method on carbonates I. Helium diffusion, Abstract #V23A-2800 presented at 2012 Fall Meeting, AGU, San Francisco, Calif.
- Pinti, D. L., Y. Gélina, M. Larocque, D. Barnette, S. Retaillieu, A. Moritz, J. F. Helie, and R. Lefebvre (2013), Concentrations, sources et mécanismes de migration préférentielle des gaz d'origine naturelle (méthane, hélium, radon) dans les eaux souterraines des Basses-Terres du Saint-Laurent, *Rep. E3–9*, 104 pp., Strategic Environ. Eval. Comm. on Shale Gas, Quebec, Canada.

- Plummer, L., and P. Glynn (2013), Radiocarbon dating in groundwater systems, in *Isotope Methods for Dating Old Groundwater*, pp. 33–90, Int. At. Energy Agency, Vienna.
- Saby, M., M. Larocque, D. L. Pinti, F. Barbecot, Y. Sano, and M. C. Castro (2016), Linking groundwater quality to residence times and regional geology in the St. Lawrence Lowlands, southern Quebec, Canada, *Appl. Geochem.*, *65*, 1–13.
- Smith, S., and B. M. Kennedy (1983), The solubility of noble gases in water and in NaCl brine, *Geochim. Cosmochim. Acta*, *47*(3), 503–515.
- Solomon, D., A. Hunt, and R. Poreda (1996), Source of radiogenic helium-4 in shallow aquifers: Implications for dating young groundwater, *Water Resour. Res.*, *32*(6), 1805–1813.
- Stute, M., and P. Schlosser (1993), Principles and applications of the noble gas paleothermometer, in *Climate Change in Continental Isotopic Records*, edited by P. K. Smart et al., *Geophys. Monogr.*, *78*, 89–100.
- Tolstikhin, I., and I. Kamenskiy (1969), Determination of ground-water ages by the T-³He method, *Geochem. Int.*, *6*, 810–811.
- Tolstikhin, I., B. Lehmann, H. Loosli, and A. Gautschi (1996), Helium and argon isotopes in rocks, minerals, and related ground waters: A case study in northern Switzerland, *Geochim. Cosmochim. Acta*, *60*(9), 1497–1514.
- Tolstikhin, I., M. Gannibal, S. Tarakanov, B. Pevzner, B. Lehmann, B. Ihly, and H. N. Waber (2005), Helium transfer from water into quartz crystals: A new approach for porewater dating, *Earth Planet. Sci. Lett.*, *238*(1–2), 31–41.
- Torgersen, T. (1980), Controls on pore-fluid concentration of ⁴He and ²²²Rn and the calculation of ⁴He/²²²Rn ages, *J. Geochem. Explor.*, *13*(1), 57–75.
- Torgersen, T., and W. B. Clarke (1985), Helium accumulation in groundwater, I: An evaluation of sources and the continental flux of crustal ⁴He in the Great Artesian Basin, Australia, *Geochim. Cosmochim. Acta*, *49*(5), 1211–1218.
- Torgersen, T., and J. O'Donnell (1991), The degassing flux from the solid earth: Release by fracturing, *Geophys. Res. Lett.*, *18*(5), 951–954.
- Torgersen, T., and M. Stute (2013), Helium (and other noble gases) as a tool for understanding long timescale groundwater transport, in *Isotope Methods for Dating Old Groundwater*, pp. 179–216, Int. At. Energy Agency, Vienna.
- Tran Ngoc, T., R. Lefebvre, E. Konstantinovskaya, and M. Malo (2014), Characterization of deep saline aquifers in the Bécancour area, St. Lawrence Lowlands, Québec, Canada: Implications for CO₂ geological storage, *Environ. Geol.*, *72*(1), 119–146.
- Vautour, G., et al. (2015), ³H/³He, ¹⁴C and (U-Th)/⁴He groundwater ages in the St. Lawrence Lowlands, Quebec, Eastern Canada, *Chem. Geol.*, *413*, 94–106.